Journal of Cerebral Blood Flow & Metabolism (2014) 34, 1463–1471

www.jcbfm.com

ORIGINAL ARTICLE

Mouse intracerebral hemorrhage models produce different degrees of initial and delayed damage, axonal sprouting, and recovery

Harriet E Barratt, Tyler A Lanman and S Thomas Carmichael

The mechanisms of delayed damage and recovery after intracerebral hemorrhage (ICH) remain poorly defined. Two rodent models of ICH are commonly used: injection of the enzyme collagenase (cICH) and injection of autologous blood (bICH). In mice, we compared the effects of these two models on initial and delayed tissue damage, motor system connections, and behavioral recovery. There is no difference in lesion size between models. Injection of autologous blood causes greater mass effect and early mortality. However, cICH produces greater edema, inflammation, and cell death. Injection of the enzyme collagenase causes greater loss of cortical connections and secondary shrinkage of the striatum. Intracerebral hemorrhage occurs within the motor system connections of the striatum. Mapping of the projections of the forelimb motor area shows a significant sprouting in motor cortex projections only in cICH. Both models of ICH produce deficits in forelimb motor control. Behavioral recovery occurs by 5 weeks in cICH and 9 weeks in bICH. In summary, cICH and bICH differ in almost every facet of initial and delayed stroke pathophysiology, with cICH producing greater initial and secondary tissue damage and greater motor system axonal sprouting than bICH. Motor recovery occurs in both models, suggesting that motor system axonal sprouting in cICH is not causally associated with recovery.

Journal of Cerebral Blood Flow & Metabolism (2014) **34,** 1463–1471; doi:10.1038/jcbfm.2014.107; published online 11 June 2014

Keywords: cell death; edema; motor; plasticity; sprouting

INTRODUCTION

Stroke is a leading cause of death and disability across the world. Intracerebral hemorrhage (ICH) constitutes up to 15% of all stroke cases, and has clinical outcomes that are often worse than ischemic stroke.[1,2] Mortality rates are as high as 50% 1 month after stroke, and survivors typically suffer life-long functional deficits.[3] Two well-established animal models of ICH are used to better understand the pathophysiology of the disease and the endogenous mechanisms of repair. These vary considerably in their mechanism. The infusion of the bacterial enzyme collagenase disrupts local blood vessels and produces endogenous hemorrhage into the site of the injection[4] but also substantial secondary inflammation.[5] Direct injection of autologous blood produces an immediate focal hemorrhage but is not derived from the native vasculature.[5,6] There have been comparative studies of these models in the rat, but no comparative studies in the mouse and no studies of the mechanisms of axonal sprouting and neural repair in experimental ICH. Axonal sprouting is a prominent feature of tissue repair and recovery in non-hemorrhagic stroke[7,8] and is causally associated with motor recovery in preclinical stroke models.[9] The present studies compare the immediate and long-term tissue damage from collagenase and autologous blood infusion models of ICH in the mouse, and the process of axonal sprouting and behavioral recovery of forelimb motor systems in this stroke subtype.

MATERIALS AND METHODS

Animals

All experiments were approved by the UCLA Chancellor's Animal Research Committee and performed in accordance with the National Institutes of Health animal protection guidelines. Two-month-old male C57/BL6 mice (Jackson Laboratories, Bar Harbor, ME, USA) were used in cohorts of 10 to 12 per group with a survival of 1 week, 5 weeks, and 9 weeks after stroke or sham procedure.

Models of Intracerebral Hemorrhage

Intracerebral hemorrhage was induced by the stereotactic injection of either autologous tail blood or of bacterial collagenase type VII (Sigma-Aldrich, St Louis, MO, USA) into the striatum. Mice were anesthetized with isoflurane and placed in a stereotaxic apparatus with constant anesthesia (1.5% to 2%) and core temperature maintained with a rectal probe ($37^\circ \pm 0.5^\circ$). Correlation between brain and core temperature was established by taking corresponding temperature readings during bICH, cICH, or sham operation ($n = 10$). A rectal probe and a brain probe (TC-100 Temperature Controller, CWE, Inc., Ardmore, PA, USA) inserted into the contralateral hemisphere were initially calibrated to ensure accurate recording. Brain and core temperatures were recorded at 5-minute intervals throughout the operation. Respiratory rate was also monitored. Animals were euthanized immediately after the operation. For the operation, the scalp was shaved, incised linearly, and a burr hole was drilled at A/P 0.95 and M/L 3.00 from bregma.

In the autologous tail blood injection (bICH), 20 μL of blood was drawn from the tip of the tail, and 12 μL of a 6:1 solution of blood with heparinized saline (1,000 units/mL saline) was loaded into a 25 μL Hamilton syringe with a 33-gauge blunt tip needle (Hamilton, Reno, NV, USA). Two successive injections were made at A/P 1.1 and A/P 0.8 to bregma. The needle was lowered at a 10° angle from the vertical to D/V −3.00 so that it would not penetrate the forelimb motor cortex. After 5 minutes, the needle was retracted to D/V −2.60 and 6 μL of autologous blood was infused at 0.5 μL/minute with two 5-minute post-injection waiting periods at D/V −2.60 and D/V −2.20 to allow for clotting. The needle was then slowly retracted, and infusion was repeated at the second injection site.

Collagenase was diluted to a stock solution 0.115 U/μL in TESCA buffer (50 mM TES buffer (*N*-tris-(hydroxymethyl)methyl-2-amino-ethanesulfonic

Department of Neurology, David Geffen School of Medicine at the University of California at Los Angeles, Los Angeles, California, USA. Correspondence: Professor Dr ST Carmichael, Department of Neurology, David Geffen School of Medicine at the University of California at Los Angeles, 710 Westwood Plaza, Los Angeles, CA 90095, USA.
E-mail: scarmichael@mednet.ucla.edu
This research was supported by NINDS NS077521.
Received 7 March 2014; revised 22 May 2014; accepted 25 May 2014; published online 11 June 2014

acid), 0.36 mM $CaCl_2$ in ddH_2O). The needle and injection approach for collagenase-induced ICH (cICH) was the same as for bICH. After 5 minutes, 0.3 μL of collagenase was infused at 0.05 μL/minute with two 2-minute post-injection waiting periods at D/V −2.60 and D/V −2.20. Sham animals underwent needle insertion but no injection.

Mapping of Motor Cortex Connections

Changes in axonal density after stroke were assessed using intracortical injection of the neuroanatomical tracer biotinylated dextran amine (BDA 10000 MW, Life Technologies, Grand Island, NY, USA). Each treatment group ($n = 10$ to 12) received an ICH or sham. Mice were injected with BDA into the forelimb motor cortex[8,9] at 4 and 8 weeks post treatment in separate cohorts. Mice were killed 1 week after BDA injection.

All brains were fixed, frozen, and coronally sectioned 50 μm apart (CM0530, Leica Biosystems, St Louis, MO, USA). A series of six sections spaced 200 μm apart were stained with Cy-5-conjugated Streptavidin (Jackson ImmunoResearch, West Grove, PA, USA), and prepared for visualization using a high-resolution Agilent DNA Microarray scanner (Agilent Technologies, Santa Clara, CA, USA). Every slide was scanned under Krypton/Argon laser at 10 μm resolution with a photomultiplier tube set at 5%. This microarray scanner measures fluorescence in a high-throughput analysis of glass slides with autofocus and a linear fluorescence quantification. Delineations of ipsilesional and contralesional striatum and cortices (ICX, CCX) were quantified (ImageJ, National Institutes of Health, Bethesda, MD, USA) for mean gray value (MGV) density profiles.

The same sections were subsequently cover slipped with Aqua-Poly/Mount (Polysciences, Warrington, PA, USA) and imaged with a Nikon C2 confocal microscope (Nikon Instruments, Melville, NY, USA) at ×10 for high-resolution BDA injection site images. Background MGV was measured for each section in the contralesional ventral cortex, which did not have axonal BDA label and reflected only background fluorescence. Individual injection volumes were determined by measuring the MGV of the ×10 injection images for the contiguous region of dense extracellular BDA, taking the sum of section means, and multiplying by 200 μm, the distance between sections. MGVs for each section were normalized to background MGV and individual injection volume.

Higher MGV means more axonal fluorescence, and indicates more axonal projections. To validate this statement from results of the microarray scans, one section from each animal was stained with Cy-3-conjugated Streptavidin (Jackson ImmunoResearch), imaged, and measured with microarray scanning as described. Then axonal projections in the contralesional striatum were then directly quantified t ×40 magnification[9] (StereoInvestigator MBF Bioscience, Williston, VT, USA) on a Leica DMLB fluorescent microscope (Leica Microsystems, Wetzlar, Germany). The microarray fluorescence intensity was correlated with the direct axonal counts (GraphPad Prism 6, La Jolla, CA, USA).

Behavior

Paw-preference was determined by the percentage of single-handed rears in the cylinder test[10,11] before ICH. Mice were categorized with preferences of left and right ($n = 10$ to 12 per group) if they exhibited >75% rears with one specific paw. Mice then received ICH/sham treatment in the hemisphere contralateral to paw-preference. Mice were tested at 1 week, 5 weeks, and 9 weeks post treatment. All behaviors were scored by observers who were masked to the treatment condition.[10,12] Grid-walking and cylinder rearing performance were assessed as described previously.[9,11,13] Mice were killed after week 9 of behavior testing.

Histology and Immunohistochemistry

Brains were fixed, frozen, and coronally sectioned at 50 μm. A series of four sections spaced 200 μm apart were stained for glial fibrillary acidic protein (GFAP, for astrocytes) and ionized calcium binding adaptor molecule 1 (Iba-1, for microglia/macrophages) as described.[8,12] Sections were blocked in 5% normal donkey serum and 0.3% Triton, and incubated with primary antibody overnight at 4 °C. Sections were then incubated with secondary antibody for 1–2 hours at room temperature, mounted on gelatin-subbed slides, dehydrated with alcohol washes, and cover slipped using DPX mounting medium (Sigma-Aldrich). Primary antibodies were goat anti Iba-1 (1:500, Abcam, Cambridge, MA, USA) and rat anti GFAP (1:500, EMD Millipore, Billerica, MA, USA). Secondary antibodies were donkey F(ab)2 fragments conjugated to Cy-2 and Cy-5 (1:500, Jackson ImmunoResearch). High-resolution ×20 confocal images and *Z*-stacks were acquired in sections double stained for GFAP and Iba-1 (C2, Nikon Instruments). Images were quantified as described[9] with MGV density profile (ImageJ, National Institutes of Health). Periinfarct MGV was normalized to the corresponding contralesional MGV. Higher MGV indicated a higher density of GFAP-positive or Iba-1-positive cells.

Terminal deoxynucleotidyl transferase dUTP nick-end labeling (TUNEL) assay was performed as described previously[12] on series of three sections using ApopTag In Situ Apoptosis Detection Kit (S7110, EMD Millipore). Briefly, sections were incubated with terminal deoxynucleotidyl transferase, which catalyzes the addition of nucleotide triphosphates labeled with digoxigenin to the 3′-OH ends of double-stranded or single-stranded DNA (which localize in apoptotic bodies in high concentrations). The digoxigenin was then detected with an antibody conjugated to fluorescein. Nuclear stains were performed by incubating the sections for 5 minutes in phosphate-buffered saline containing propidium iodide before cover slipping. Cell nuclei tagged by TUNEL were manually quantified using neuroanatomical quantification software (StereoInvestigator, MBF Bioscience).

For mapping of Cholera Toxin Subunit B-injected brains, at the time of ICH induction, 0.5 μL of retrograde neuronal tracer Cholera Toxin Subunit B (CTb, List Biological Laboratories, Campbell, CA, USA, diluted to 20 μg/μL in 10% DMSO) was infused with collagenase, blood, or alone. Seven days after treatment, animals were killed, and brains were fixed, frozen, and coronally sectioned at 50 μm. A series of six sections spaced 200 μm apart were blocked in 5% normal donkey serum and 0.3% Triton, incubated with a CTb primary antibody (Goat anti-CTb, 1:500, List Biological Laboratories) overnight, and incubated with a secondary antibody (Donkey anti-goat conjugated to Cy3, 1:500, Jackson ImmunoResearch) for 1 hour. Sections were mounted, cover slipped, and visualized under the Cy3 filter on a DMLB epifluorescent microscope (Leica Microsystems). Cortical cells labeled with CTb were manually quantified using neuroanatomical quantification software (StereoInvestigator, MBF Bioscience).

Lesion or infarct size was measured in tissue sections stained with Cresyl violet.[14] Images at ×4 magnification were acquired (SPOT 5.0, Diagnostic Instruments, Sterling Heights, MI, USA) in six 50-μm sections spaced 200 μm apart and area measurements of infarct, hemisphere, striatum, and ventricle were quantified using ImageJ software. Hemorrhagic injury volume was computed by summation of the infarct areas multiplied by the inter-slice distance of 200 μm. Ventricle dilation and striatal deterioration were measured on the basis of percent ventricular enlargement, and percent striatal shrinkage compared with the contralateral hemisphere.

Brain edema was measured using the wet/dry weight method as previously described.[15] Briefly, animals ($n = 20$) were euthanized, and the brain was removed and dissected into the left and right hemisphere. The cerebellum was kept as an additional control. Tissue samples were rapidly weighed with a basic precision scale (APX-153, Denver Instruments, Bohemia, NY, USA) and dried for 24 hours in a vacuum oven at 80 °C. The percent brain water in each tissue sample was calculated according the following equation: %water = ((wet weight − dry weight)/wet weight) × 100%.

The hemoglobin content of brains subjected to bICH, cICH, or sham ($n = 18$) was quantified with a spectrophotometric assay as previously described.[16] Briefly, animals were euthanized, and the brain was removed and dissected into the left and right hemisphere. Distilled water (250 μL) was added to each tissue sample, followed by homogenization for 1 minute and centrifugation at 13,000 r.p.m. for 30 minutes. After the hemoglobin-containing supernatant was collected, 100 μL of Drabkin's reagent (Sigma-Aldrich, $K_3Fe(CN)_6$ 200 mg/L, KCN 50 mg/L, $NaHCO_3$ 1 g/L, pH 8.6) was added to a 25 μL aliquot and allowed to stand for 15 minutes. This reaction converts hemoglobin to cyanomethemoglobin, which has an absorbance peak at 540 nm. Optical density was measured at a wavelength of 540 nm with a spectrophotometer. Results from three samples per mouse were averaged. To verify that the measured absorbance reflected the amount of hemoglobin, blood was obtained from naïve mice by cardiac puncture after anesthesia. Incremental aliquots of this blood (0, 1, 2, 4, 8, and 16 μL) were added to freshly homogenized brain tissue from untreated mice to generate a standard absorbance curve. This curve showed a linear relationship between added blood and optical density. The ratio of hemoglobin content was calculated according to the following equation: ratio = (ipsilesional hemisphere/contralesional hemisphere).

Statistical Analysis

All tests were analyzed blindly to experimental condition. Animals were randomly assigned to treatment condition. Sample size was determined by

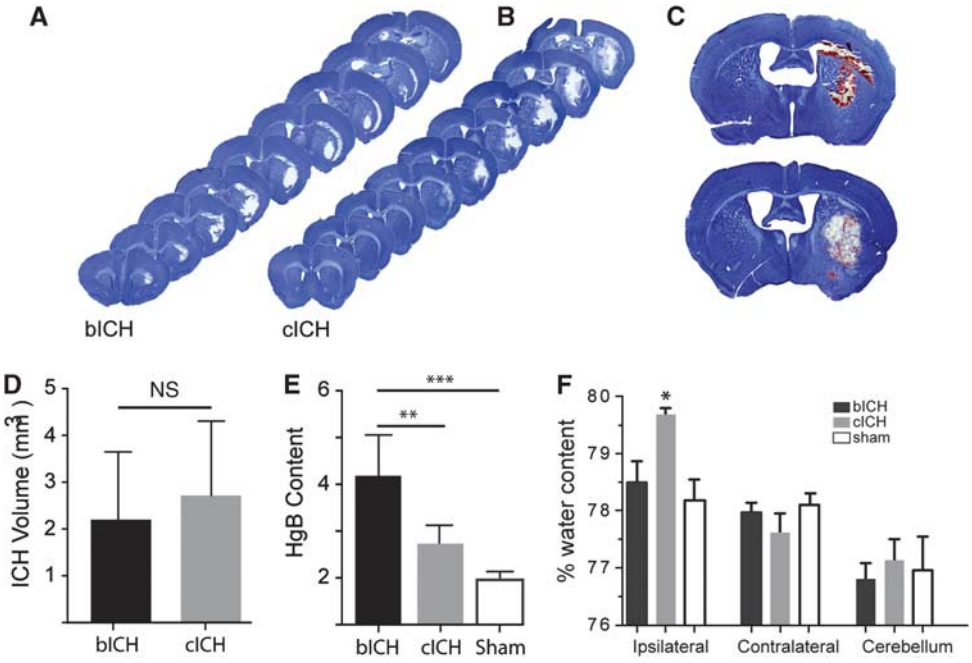

Figure 1. Initial tissue damage after intracerebral hemorrhage (ICH). (**A**, **B**) Representative images of hemorrhage at 24 hours post ICH show a similar distribution and size of damage in the two hemorrhage models. There is no significance between autologous blood intracerebral hemorrhage (bICH) and collagenase intracerebral hemorrhage (cICH) at any coronal level, indicating similar lesion location. (**C**) Differences in blood density are visually apparent between the bICH and cICH 24 hours after ICH. (**D**) There is no difference between the sizes of the lesion at 24 hours in the two models. ($n = 13$, bICH $= 2.201\ mm^3 \pm 1.362$, cICH $= 2.716\ mm^3 \pm 1.560$) (**E**) Hemoglobin content (Hgb) as expressed in ispilesional/contralesional spectroscopic readings. (bICH $= 3.843 \pm 1.058$, cICH $= 2.069 \pm 0.492$, sham $= 1.186 \pm 0.214$, $n = 16$, $^{**}P < 0.01$, $^{***}P < 0.001$.) (**F**) Brain edema is expressed as the % water content in the cerebral hemisphere ipsilateral or contralateral to the hemorrhage or in the cerebellum. The brain edema is significantly greater in cICH than all other groups at 3 days post stroke ($n = 17$, $^{*}P < 0.05$ ipsilateral versus contralateral cICH). NS, nonsignificant.

a power analysis (Statistical Solutions, Cottage Grove, WI, USA), with the expected variance and change in performance in the grid-walking and cylinder rearing tasks predicted based on published studies.[8–10,13] A group size of $n = 10$ was predicted to be sufficient to detect a statistically significant result in analysis of variance with $\alpha = 0.05$ and power > 0.8. No animals were excluded from the analyses in these studies. All data are expressed as mean ± s.d. For axonal quantification, specific structural measurements, and behavioral testing, differences between treatment groups were analyzed using two-way analysis of variance corrected for multiple comparisons, with Tukey–Kramer *post hoc* testing. Statistical differences in mortality rate were determined using χ^2 analysis (all statistics performed with GraphPad Prism 6).

RESULTS

Infarct Volume and Tissue Damage

There is no difference in lesion size between ICH models 24 hours after stroke ($n = 13$, bICH $= 2.201\ mm^3 \pm 1.362$, cICH $= 2.716\ mm^3 \pm 1.560$, Figures 1A–C), and no significant difference between bICH and cICH at any coronal level through the lesion, indicating similar lesion location as well as size (Supplementary Figure 1D). The methodology for producing the hemorrhage did not generate differences in physiologic variables, such as brain or body temperature or respiratory rate (Supplementary Figure 1A). Brain and body temperature was highly correlated ($R^2 = 0.7156$, $n = 10$). This equivalency in lesion size means that observations on tissue damage and reorganization are likely influenced by the model mechanism, rather than the size of the lesion. The hemorrhagic area is visibly denser in autologous blood ICH (bICH) than in collagenase ICH (cICH) (Figure 1D), indicating a region of bland infarcted tissue in the cICH model. This is confirmed by measuring hemoglobin content from brains with bICH, cICH and sham, with bICH having significantly greater amounts of hemoglobin in the same lesion volume (Figure 1E, bICH $= 3.843 \pm 1.058$, cICH $= 2.069 \pm 0.492$, sham $= 1.186 \pm 0.214$, $n = 16$, $^{**}P < 0.01$, $^{***}P < 0.001$). The reduced blood content in cICH, but same lesion size as bICH, indicates that cICH produces hemorrhage plus bland (non-hemorrhagic) stroke, which is apparent in tissue sections from cICH (Figure 1C). Autologous blood ICH is produced with trace heparinized saline, to prevent clotting of autologous blood between collection and injection into the brain. Hemoglobin content was compared from bICH with cICH and with cICH with trace heparinized saline added to the collagenase. However, there was no difference in hemoglobin content between cICH and cICH with trace heparin, so these two groups were combined in the statistical analysis.

Progressing damage was measured in both models. Hemispheric enlargement was greater in bICH, peaking at 3 days (Supplementary Figure 1E, $n = 21$, $^{*}P < 0.05$, $^{**}P < 0.01$, 1st day: bICH $= 3.70\% \pm 3.77$, cICH $= 3.68\% \pm 3.04$, sham $= -0.4\% \pm 2.05$, 3rd day: bICH $= 6.47\% \pm 4.24$, cICH $= -1.14\% \% \pm 4.14$, sham $= 2.26\% \pm 2.57$). Although brain edema was seen in both models, only cICH showed significantly increased brain edema at 3 days (Figure 1F). This indicates that the hemispheric enlargement in bICH is due to mass effect from the blood but not to edema. Also, total mortality of mice, with deaths occurring exclusively in the first 48 hours after ICH, differed between the experimental models. While no mouse died in the sham group, overall mortality was 5.6% in cICH and 12.5% in bICH ($^{*}P < 0.05$, $n = 127$, Supplementary Figure 1A). Mice which died post operation were excluded from all further experiments. No animal death occurred more than 48 hours after stroke. Both ICH models were associated with moderate weight loss compared with sham-operated mice (Supplementary Figure 1B).

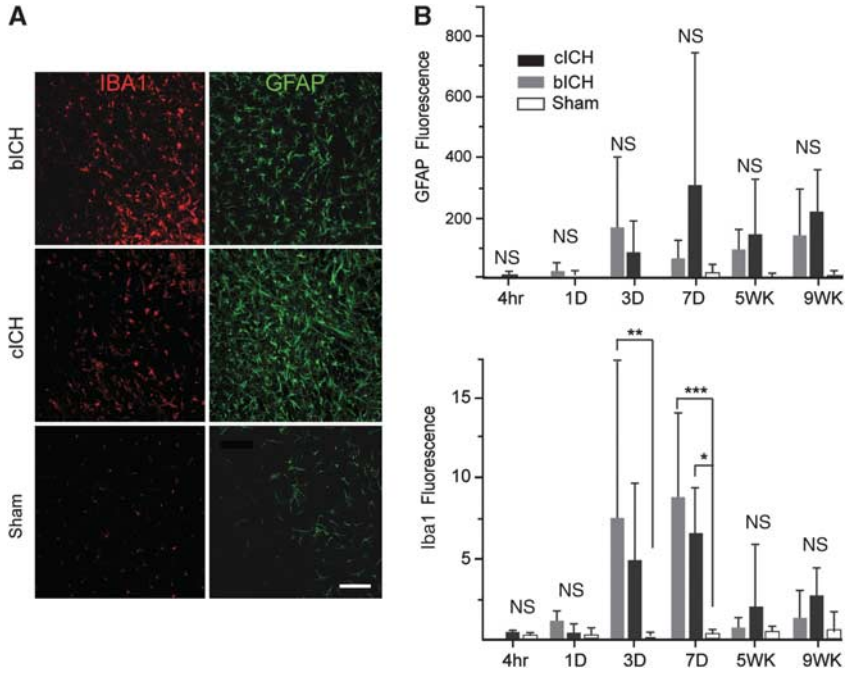

Figure 2. Inflammatory and astrocyte responses after intracerebral hemorrhage (ICH). (**A**) Iba-1-positive microglia/macrophages (red) and glial fibrillary acidic protein (GFAP)-positive astrocytes (green) are visible in the perihematomal striatum in both autologous blood intracerebral hemorrhage (bICH) and collagenase intracerebral hemorrhage (cICH) at 7 days after stroke. (**B**) Quantification of the GFAP And Iba-1 immunoreactivity indicated that the increase in GFAP staining did not reach significance but the Iba-1 staining was greater at day 7 in bICH and cICH ($n = 4$ per group, $^{*}P < 0.05$, $^{**}P < 0.01$, $^{***}P < 0.001$). Scale bar, 100 μm. NS, nonsignificant.

Inflammation, Gliosis Cell Death, and Axonal Loss after Intracerebral Hemorrhage

The inflammatory response to ICH was assessed at multiple time points after stroke. Iba-1 staining for microglia/macrophages after ICH showed an increase in staining in both models at 3 and 7 days, that is significantly increased compared with sham injection at 7 days (Figures 2A and 2B, $n = 4$ per group, $^{*}P < 0.05$, $^{**}P < 0.01$, $^{***}P < 0.001$), with a greater increase in cICH. An increase in GFAP staining for astrocytes was seen at 1, 5, and 9 weeks after stroke. There is substantial variability in GFAP staining after ICH. Although it did not reach significance, cICH showed a higher level of GFAP immunoreactivity around the hemorrhage cavity than bICH (Figures 2A and 2B). Power analyses indicate that variation in GFAP staining across treatment groups is such that a sample size of over 30 in each group (540 for the entire study) would be necessary to detect a significant difference in GFAP staining.

Terminal deoxynucleotidyl transferase dUTP nick-end labeling staining 24 hours after stroke revealed extensive cell death throughout the infarct core, especially in cICH (Figures 3A and 3B). The number of TUNEL + cells did not differ between bICH and sham groups at the 24-hour time point (Figures 3A and 3C) but was significantly higher in cICH ($^{**}P < 0.01$, $n = 16$). Seven days and 21 days after ICH, there are elevated levels of TUNEL + cells in cICH and bICH, but these are not significantly different from sham (Figure 3C). Note that the sham condition in all of these studies is needle placement alone (without blood or collagenase injection) into the striatum, which produces this low level of observed cell death. In bICH and cICH, TUNEL + cells were found in the infarct core and adjacent periinfarct areas (Figure 3B). Intracerebral hemorrhage in humans produces significant, delayed tissue atrophy.[17,18] In mouse ICH, a decrease in ipsilesional striatum size was seen in both ICH models after 9 weeks, with significantly greater striatal shrinkage compared with sham in cICH (Figure 3D, $^{**}P < 0.01$, $n = 12$). The cICH model also showed ipsilesional ventricular dilation after 9 weeks. Thus, both models produce initial cell death, but this is of greater magnitude in cICH and results in greater long-term tissue atrophy in this model.

In human and rodent ICH, the striatum is the predominant location of damage.[19] It is also a site of termination of axonal projections from cortex and a passage point where cortical projections pass through to thalamus, brainstem, and spinal cord.[20,21] Intracranial hemorrhage damages these connections.[22] The degree of loss of cortical projections to or through the striatum was measured by back-labeling all of the cortical axons that project to the site of the ICH with the axonal tracer CTb, within the collagenase or blood injection, and then measuring the retrogradely labeled cell bodies. This approach labels cells that project to or through the hemorrhagic lesion,[23] allowing a quantification of the effect of the ICH on network connectivity of the overlying cortex. A large number of neurons in cingulate, frontal, and parietal cortex of both hemispheres project to the site of the ICH (Figures 4A and 4B). These include primary motor and somatosensory areas and secondary somatosensory areas bilaterally. There is a significant loss of cortical projections after ICH, particularly cICH. Collagenase-induced ICH causes loss of cortical projections from cortex ipsilateral and contralateral to the hemorrhage (Figure 4, $^{*}P < 0.05$, $^{***}P < 0.001$, $n = 12$). Autologous blood ICH causes a less significant loss of projections only from contralateral cortex.

Motor Impairments after Intracerebral Hemorrhage

Forelimb motor performance was assessed in both models. Animals performed similarly in a prestroke assessment of both grid-walking and cylinder rearing tasks. One week after stroke, bICH and cICH showed a significant motor deficit indicated by an increase in forelimb foot faults in the grid-walking task compared with baseline levels (Figure 5, $^{**}P < 0.01$, $^{***}P < 0.005$, $n = 32$). By 5 weeks post stroke, functional recovery occurred in cICH, while there was still a significant motor deficit seen in bICH (Figure 5,

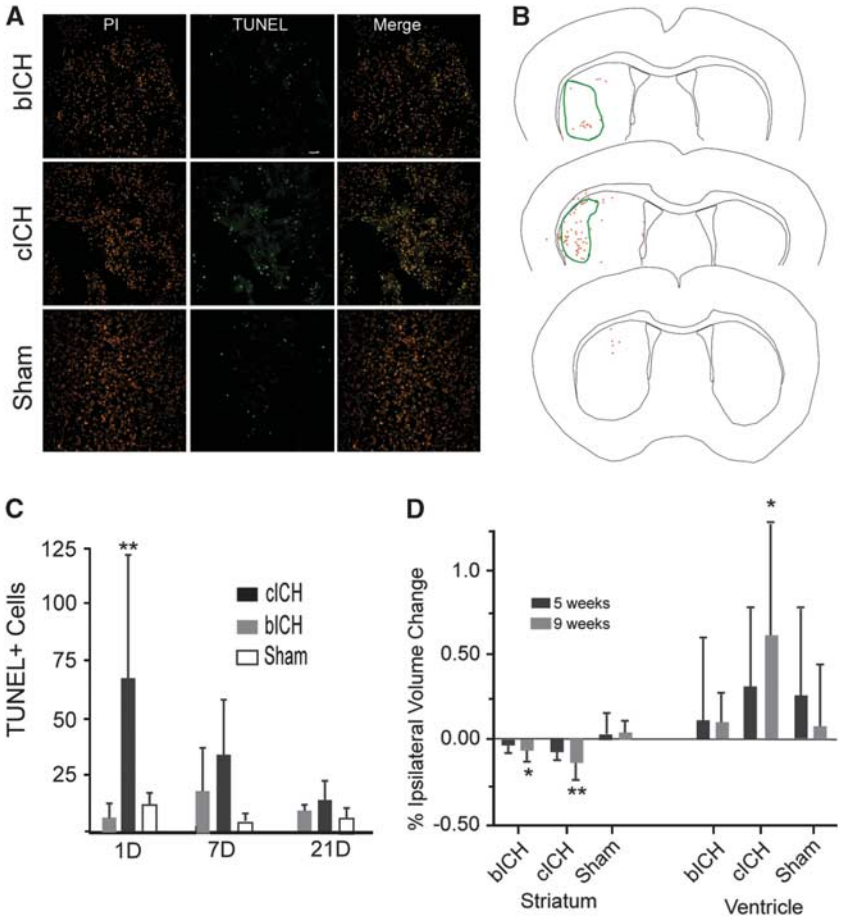

Figure 3. Cell death after intracerebral hemorrhage (ICH). (**A**) Terminal deoxynucleotidyl transferase dUTP nick-end labeling (TUNEL)-positive cells (green) localize to the infarct core 24 after stroke in collagenase intracerebral hemorrhage (cICH). Cell nuclei are stained with propidium iodide (red). Scale bar, 200 μm. An increased number of dead cells are seen in cICH 24 hours after stroke. (**B**) Maps of TUNEL+ cells (red asterisks) in coronal sections at the level of the ICH (green line) in autologous blood intracerebral hemorrhage (bICH) (top), cICH (middle), and sham (bottom). (**C**) Quantification of TUNEL+ cells after ICH. Cell death is still visible in both bICH and cICH at 7 days after stroke. (**$P<0.01$ compared with sham and bICH, $n=16$). (**D**) Tissue atrophy after ICH. Collagenase intracerebral hemorrhage showed significant striatal shrinkage after 9 weeks ($n=12$, *$P<0.05$, **$P<0.01$), and also showed higher ipsilesional ventricle dilation, although not significant.

**$P<0.01$). Gait in the bICH model returned to baseline performance by 9 weeks post ICH. The cylinder rearing task suggested an increased motor deficit in both models at 1 week and 5 weeks, although this was not significant.

Motor System Connections after Intracerebral Hemorrhage

Motor cortical projections have an important role in motor function and movement. In human and rodent ICH, the hemorrhage site is in the region of motor cortex projections within the ipsilateral hemisphere and from the ipsilateral hemisphere to contralateral cortex and striatum,[21]. The anatomical tracer BDA was injected into forelimb motor cortex[24] 8 weeks after ICH. The axons were visualized with fluorescent labeling using a linear fluorescent high-resolution microarray scanner. To first determine that this measurement accurately and linearly measures axonal projections, BDA-labeled axons were counted and regressed with fluorescent measurements in the same area for all animals in this study (Supplementary Figure 2A). A statistically significant, linear correlation was shown between microarray scanner fluorescent intensity and number of axons, validating the accuracy of the microarray data ($n=29$, $r^2=0.6442$, Supplementary Figure 2B). There is moderate axon density loss in both bICH and cICH at 5 weeks post stroke compared with sham (Figure 6B, CCX: bICH $=0.200\pm0.205$, cICH $=0.203\pm0.164$, sham $=0.443\pm0.389$, contralesional striatum: bICH $=0.092\pm0.111$, cICH $=0.109\pm0.099$, sham $=0.184\pm0.179$, ICX: bICH $=1.313\pm1.604$, cICH $=1.564\pm1.401$, sham $=2.013\pm1.575$, ipsilesional striatum: bICH $=1.118\pm1.638$, cICH $=1.448\pm1.176$, sham $=1.573\pm1.365$).

At 9 weeks, corticostriatal projections are significantly increased in cICH compared with 5 weeks. Axonal density increased approximately fourfold in both the ipsilesional cortex and striatum, and over 10-fold in the contralesional cortex and striatum (Figures 6A and 6B). In the sham model, axonal labeling was similar between time points. While the bICH model showed the same increasing trends for motor system axonal connection as cICH, the changes in axonal density did not reach significance (Figure 6, CCX: bICH $=1.775\pm2.304$, cICH $=2.514\pm0.2.259$, sham $=0.753\pm0.968$, contralesional striatum: bICH $=0.982\pm1.333$, cICH $=1.916\pm1.554$, sham $=0.377\pm0.617$, ICX: bICH $=3.974\pm4.581$, cICH $=6.535\pm6.269$, sham $=1.926\pm2.386$, ipsilesional striatum: bICH $=2.375\pm3.105$, cICH $=5.199\pm4.701$, sham $=1.547\pm2.701$). Thus, cICH produces a significant axonal sprouting response from the ipsilateral cortex (above the ICH) to both the contralateral and ipsilateral cortex and striatum.

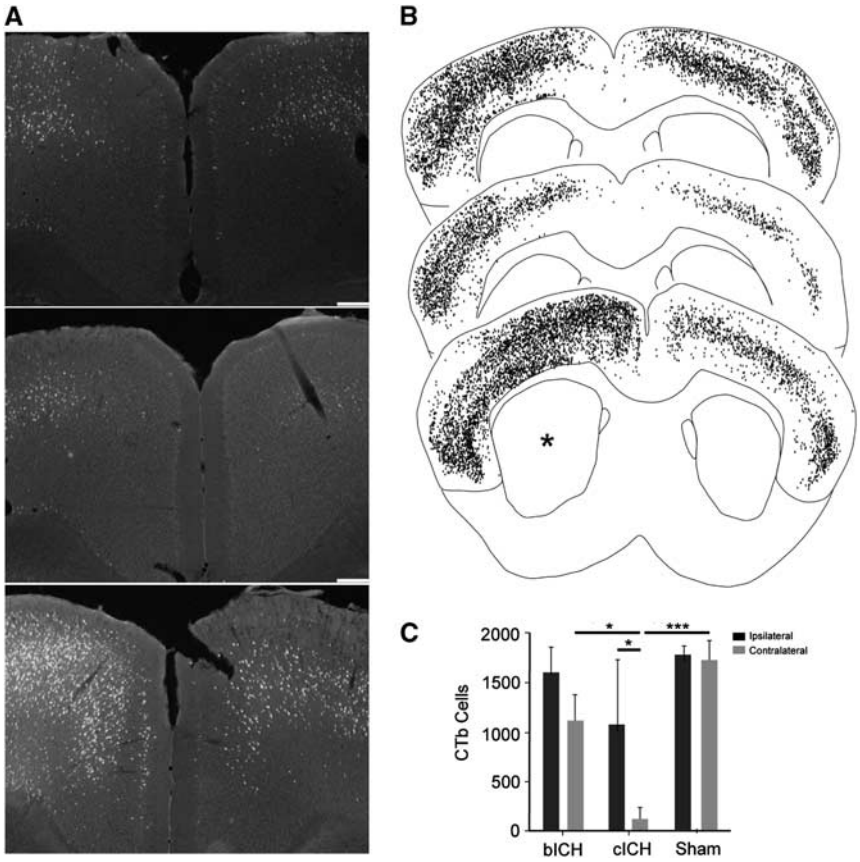

Figure 4. Axonal connections with striatum after intracerebral hemorrhage (ICH). (**A**) Representative photomicrographs of cingulate cortex from sham (top), collagenase intracerebral hemorrhage (cICH) (middle) and autologous blood intracerebral hemorrhage (bICH) (bottom). Cells labeled with Cholera Toxin Subunit B (CTb) are bright against the dark tissue background. Scale bar, 200 μm. (**B**) Digital plots of CTb-labeled cells in coronal sections from sham (top), cICH (middle) and bICH (bottom). Each dot is one cell. Asterisk shows side of ICH. (**C**) Quantification of cortical cells that project to striatum. There is a significant loss of cortical projections after cICH. ($n = 12$, $^{*}P < 0.05$, $^{****}P < 0.0001$).

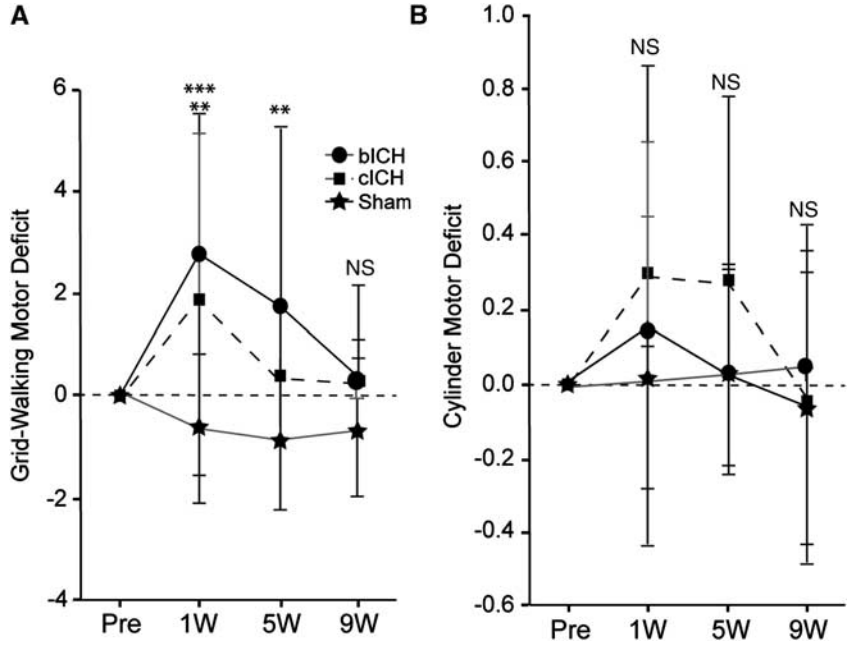

Figure 5. Motor impairments after intracerebral hemorrhage (ICH). (**A**) In the grid-walking test, autologous blood intracerebral hemorrhage (bICH) and collagenase intracerebral hemorrhage (cICH) showed significant foot faults of the contralateral forelimb 1 week after ICH. While cICH recovered to baseline performances by 5 weeks after ICH, bICH still exhibited motor deficits. Both groups performed at baseline levels by 9 weeks after stroke. (**B**) The cylinder rearing task suggested an increased motor deficit in both models at 1 week and 5 weeks, which was not significant ($^{**}P < 0.01$, $^{***}P < 0.001$, $n = 32$). NS, nonsignificant.

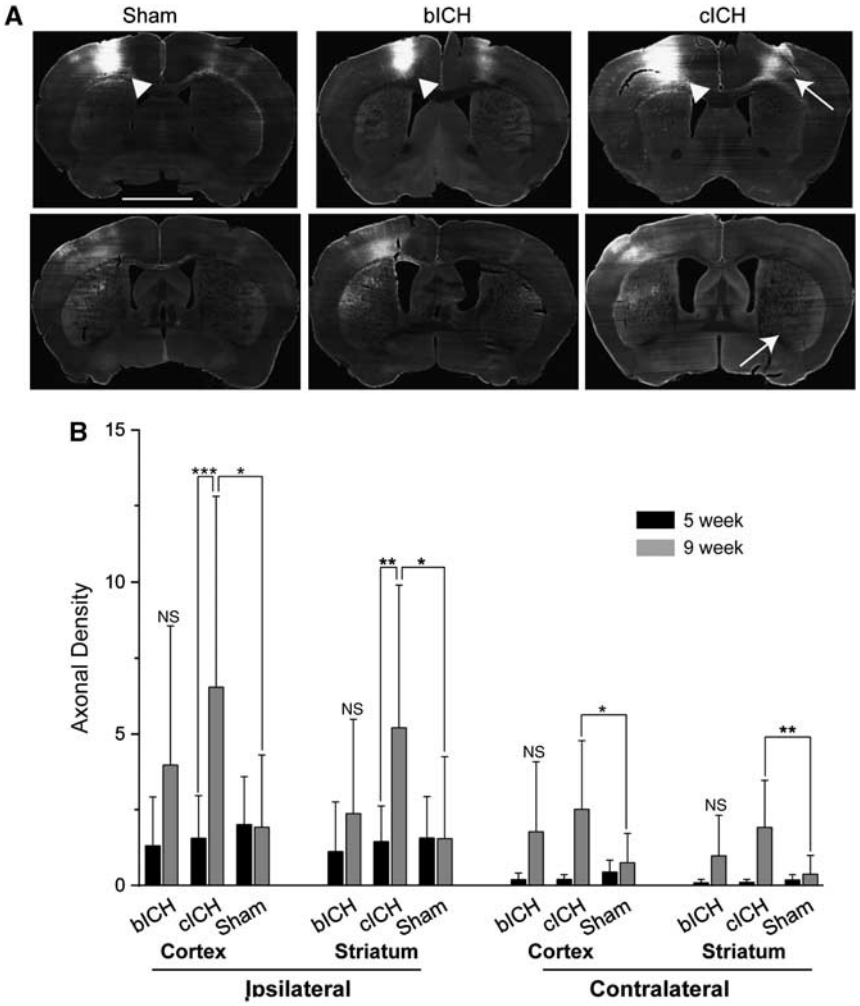

Figure 6. Motor cortex connections after intracerebral hemorrhage (ICH). (**A**) Images of biotinylated dextran amine (BDA)-labeled connections from motor cortex. Bright label represents labeled axons from and to the injection site. Arrowheads show injection site in the motor cortex. Arrows show contralateral cortex and striatum projections in collagenase intracerebral hemorrhage (cICH) condition. (**B**) Quantification of axonal projections. Streptavidin staining of anterograde BDA shows increased axonal density in cICH at 9 weeks compared with 5 weeks. There was a significant increase in axon density in cICH compared with sham in the both contra- and ipsilesional striatum and cortex. ($n = 32$, $^{*}P < 0.05$, $^{**}P < 0.01$, $^{***}P < 0.001$). bICH, autologous blood intracerebral hemorrhage; NS, nonsignificant.

DISCUSSION

The development of novel therapeutics to support repair after stroke and ICH is dependent on accurate animal modeling of the disease. This study performed a direct comparison of tissue damage and long-term neurologic function in the two most widely used models of experimental ICH in the mouse, collagenase ICH (cICH) and autologous blood ICH (bICH). The two ICH methods produce equivalent lesion sizes. Collagenase intracerebral hemorrhage produces a lesion that more closely matches a hemorrhagic stroke, with bland tissue and less blood in the same-sized lesion cavity. Despite this equivalency in lesion size, cICH produces greater cell death, edema, inflammation, and delayed ventricular dilation, and bICH produces greater initial mass effect from the blood and higher mortality. Both types of hemorrhage destroy axonal projections to the striatum, but this loss was dramatic in cICH, with loss of over 95% of the projections from the cortex contralateral to the striatal hemorrhage site. Both models produced forelimb motor control deficits, with those in cICH recovering at 5 weeks and those in bICH recovering by 9 weeks. New motor projections form between 5 and 9 weeks in cICH from forelimb motor cortex to ipsilateral and contralateral cortical and striatal areas. This difference in tissue damage and long-term axonal sprouting patterns indicates that the two models used in ICH differ in almost every facet of initial and delayed effects of stroke and of reactive plasticity in the post-stroke brain.

In the present study, we modified injection of autologous blood and collagenase for the ICH. Initially, these ICH models were developed so the blood or the collagenase was injected directly down into the targeted brain area, the striatum.[25] However, these coordinates cause the needle to penetrate the mouse forelimb motor cortex, causing damage to this primary motor region and complicating the interpretation of a motor deficit, as the motor deficit may be due to the hemorrhage in the striatum or to the damage in the motor cortex from the needle en route to the striatum. To resolve this complication, the injection was done at a 10° angle, with the needle tract not passing through the forelimb motor cortex. We further improved the previous models of ICH by administering blood or collagenase via a smaller, 33-gauge needle. This modification prevented backflow commonly seen, especially in bICH, and further minimized damage from the technique itself outside of the hemorrhage site. This revised method in both models of ICH produced lesions that did not differ in size at any anterior/posterior level. The use of heparin in bICH did not induce additional bleeding when added as a test to the

cICH model, but it may be associated with other effects not studied here. Both lesions targeted the dorsolateral striatum, the site of sensorimotor system function.[20,21] However, although these lesions overlap across animals in their location within the dorsolateral striatum of the mouse, their precise anatomic positions were not matched.

Previous studies have compared collagenase and blood ICH models in the rat. The differences in the rat between these two models parallel many of those in the mouse. As in the present findings in the mouse, rat cICH produces greater edema, local neuronal loss in the striatum, and greater tissue atrophy; inflammation is more pronounced in the rat cICH model.[26,27] As in the present study, the cylinder test of forelimb function shows a very modest cylinder effect in cICH in rats[28] or a short-term effect in cICH in mice.[29] Some of the effects of bICH and cICH in the mouse are distinct to that seen in the rat. Behavioral deficits persist for a greater period in rat cICH[26,30] than in the mouse. Unlike in rat, sensorimotor deficits as measured by gait in the mouse resolve sooner in cICH than bICH. These two lesions models also have very distinct patterns of axonal loss and later axonal sprouting.

One of the main findings in this study is that there is a difference in axonal loss, long-term atrophy, and secondary axonal sprouting between cICH and bICH despite similarly sized lesions. Collagenase intracerebral hemorrhage produces greater shrinkage of the striatum and ventricular dilation than bICH. In fact, there is no difference in bICH in the striatal or ventricular size compared with sham. Collagenase intracerebral hemorrhage causes significantly greater loss of cortical projections, particularly in the projections from the somatosensory and motor cortical areas contralateral to the striatum, which are nearly completely lost after cICH. In rat cICH, there is loss of connections to the striatum with a modest reduction in neurons that project from the substantia nigra to the striatum,[31] a decrease in cortical projections from the ipsilateral motor cortex[32] and thinning of ipsilateral cortex.[26] There are no reports of axonal loss in the rat in bICH. This greater loss of axonal projections to the striatum in cICH in the mouse could be due to greater local tissue damage after the hemorrhage. Although the lesion size did not differ between the two models, there is greater cell death in hemorrhage tissue in cICH, edema, and inflammation. These may be measures of incomplete damage in apparently intact tissue adjacent to the hemorrhage after collagenase injection, rather than in autologous blood injection. This greater incomplete damage in perihematomal tissue in cICH is likely because damage in cICH reflects both hemorrhage and also bland (non-hemorrhagic) stroke (Figures 1C and 1E). In rat cICH, myelin is damaged and myelin debris is present 1 to 3 days after ICH in the margins of the hematoma and adjacent perihematomal tissue.[14] Axonal damage, as assessed by axonal accumulation of beta-amyloid precursor protein, retraction bulbs, and disintegrating axonal profiles, is seen in the first 3 days after cICH in the rat adjacent to the hemorrhage.[14] The present and published data suggest that cICH produces greater tissue injury in perihematomal striatum and that this leads to greater secondary tissue atrophy and loss of projections to the striatum from cortex.

This is the first report of spontaneous axonal sprouting after ICH. While there is an increase in axonal projections from the forelimb motor cortex ipsilateral to the lesion in both models, this was only significant for cICH. In fact, cICH produces dramatic axonal sprouting from the forelimb motor cortex above the striatal hemorrhage, such that there is a three to fivefold increase in axonal projections from motor cortex. Axonal sprouting occurs in non-hemorrhagic stroke, from cortex opposite to the stroke to striatum, brainstem, and spinal cord and in the cortex adjacent to the stroke.[7] In the cortex adjacent to the stroke, axonal sprouting forms new projections that link motor cortex to premotor and somatosensory areas.[8] When the formation of these new projections from motor adjacent to the stroke to premotor cortex is blocked, mice do not experience motor recovery.[9] These data establish a causal role for post-stroke axonal sprouting in behavioral recovery in some mouse stroke models. In cICH, post-hemorrhage axonal sprouting occurred between 5 and 9 weeks after the hemorrhage was induced. This means that axonal sprouting occurred after mice had recovered motor function, which occurred at 5 weeks after hemorrhage. Further, mice with cICH and bICH recovered to the same behavioral performance despite the very different degrees of axonal sprouting between these two ICH models. The inference here is that axonal sprouting in cICH, unlike that seen in non-hemorrhagic stroke in the mouse, is not associated with functional recovery.

Human ICH results in disconnection syndromes in overlying cortex, and recovery is associated with the strength of functional connectivity in sensorimotor areas. Patients with ICH in the striatum show lower measures of connectivity from the ipsilateral hand motor cortex to contralateral motor, striatal/basal ganglial and subcortical sites.[33,34] This parallels cICH in the present study, where connections from the mouse forelimb motor cortex ipsilateral to the lesion drop out after the hemorrhage. These parallels between connectivity patterns in human ICH and mouse cICH raise the important issue of which mouse ICH model might be considered to most closely model the human condition. Damage after ICH in humans can occur with local displacement of brain structures from blood, mass effect from edema, and toxicity of blood breakdown products.[2] Edema after ICH produces a high early mortality.[2] The initial mass effect and higher mortality in mouse bICH models these early events in human ICH. However, in mouse cICH, there is greater overall tissue damage and a component of non-hemorrhagic stroke. Thus, the pattern of atrophy and loss of connections would suggest that cICH produces a pattern of injury seen in more severe human ICH and bICH produces a pattern of damage seen in less severe ICH. However, functional recovery occurs in both models. Thus, there are four conclusions from detailed studies of mouse ICH models: cICH produces a pattern of damage and disconnection that models moderate to severe human ICH; bICH produces a pattern of initial lesion progression that models human ICH; the patterns of behavioral recovery in the mouse are disassociated from the underlying brain damage; and reactive axonal sprouting in cICH is not linked to functional recovery.

DISCLOSURE/CONFLICT OF INTEREST

The authors declare no conflict of interest.

REFERENCES

1 Broderick JP, Adams HP Jr, Barsan W, Feinberg W, Feldmann E, Grotta J *et al.* Guidelines for the management of spontaneous intracerebral hemorrhage: a statement for healthcare professionals from a special writing group of the Stroke Council, American Heart Association. *Stroke* 1999; **30**: 905–915.
2 Qureshi AI, Mendelow AD, Hanley DF. Intracerebral haemorrhage. *Lancet* 2009; **373**: 1632–1644.
3 Aronowski J, Hall CE. New horizons for primary intracerebral hemorrhage treatment: experience from preclinical studies. *Neurol Res* 2005; **27**: 268–279.
4 Masuda T, Maki M, Hara K, Yasuhara T, Matsukawa N, Yu S *et al.* Peri-hemorrhagic degeneration accompanies stereotaxic collagenase-mediated cortical hemorrhage in mouse. *Brain Res* 2010; **1355**: 228–239.
5 Xue M, Del Bigio MR. Comparison of brain cell death and inflammatory reaction in three models of intracerebral hemorrhage in adult rats. *J Stroke Cerebrovasc Dis* 2003; **12**: 152–159.
6 Sansing LH, Kasner SE, McCullough L, Agarwal P, Welsh FA, Kariko K. Autologous blood injection to model spontaneous intracerebral hemorrhage in mice. *J Vis Exp* 2011, pii: 2618; doi:10.3791/2618.
7 Benowitz LI, Carmichael ST. Promoting axonal rewiring to improve outcome after stroke. *Neurobiol Dis* 2010; **37**: 259–266.
8 Li S, Overman JJ, Katsman D, Kozlov SV, Donnelly CJ, Twiss JL *et al.* An age-related sprouting transcriptome provides molecular control of axonal sprouting after stroke. *Nat Neurosci* 2010; **13**: 1496–1504.

9 Overman JJ, Clarkson AN, Wanner IB, Overman WT, Eckstein I, Maguire JL *et al.* A role for ephrin-A5 in axonal sprouting, recovery, and activity-dependent plasticity after stroke. *Proc Natl Acad Sci USA* 2012; **109**: E2230–E2239.
10 Clarkson AN, Huang BS, Macisaac SE, Mody I, Carmichael ST. Reducing excessive GABA-mediated tonic inhibition promotes functional recovery after stroke. *Nature* 2010; **468**: 305–309.
11 Baskin YK, Dietrich WD, Green EJ. Two effective behavioral tasks for evaluating sensorimotor dysfunction following traumatic brain injury in mice. *J Neurosci Methods* 2003; **129**: 87–93.
12 Rosenzweig S, Carmichael ST. Age-dependent exacerbation of white matter stroke outcomes: a role for oxidative damage and inflammatory mediators. *Stroke* 2013; **44**: 2579–2586.
13 Clarkson AN, Overman JJ, Zhong S, Mueller R, Lynch G, Carmichael ST. AMPA receptor-induced local brain-derived neurotrophic factor signaling mediates motor recovery after stroke. *J Neurosci* 2011; **31**: 3766–3775.
14 Wasserman JK, Schlichter LC. White matter injury in young and aged rats after intracerebral hemorrhage. *Exp Neurol* 2008; **214**: 266–275.
15 Xi G, Keep RF, Hoff JT. Erythrocytes and delayed brain edema formation following intracerebral hemorrhage in rats. *J Neurosurg* 1998; **89**: 991–996.
16 Choudhri TF, Hoh BL, Solomon RA, Connolly ES Jr, Pinsky DJ. Use of a spectrophotometric hemoglobin assay to objectively quantify intracerebral hemorrhage in mice. *Stroke* 1997; **28**: 2296–2302.
17 Skriver EB, Olsen TS. Edema and atrophy following cerebral stroke. A prospective and consecutive study. *Acta Radiol Suppl* 1986; **369**: 43–45.
18 Brander A, Kotila M, Salonen O. Spin-echo MRI of chronic intracerebral haematomas. *Neuroradiology* 1997; **39**: 25–29.
19 Hill MD, Silver FL, Austin PC, Tu JV. Rate of stroke recurrence in patients with primary intracerebral hemorrhage. *Stroke* 2000; **31**: 123–127.
20 Doig NM, Moss J, Bolam JP. Cortical and thalamic innervation of direct and indirect pathway medium-sized spiny neurons in mouse striatum. *J Neurosci* 2010; **30**: 14610–14618.
21 Shepherd GM. Corticostriatal connectivity and its role in disease. *Nat Rev Neurosci* 2013; **14**: 278–291.
22 McDowell MM, Kellner CP, Barton SM, Mikell CB, Sussman ES, Heuts SG *et al.* The role of advanced neuroimaging in intracerebral hemorrhage. *Neurosurgical focus* 2013; **34**: E2.
23 Sozmen EG, Kolekar A, Havton LA, Carmichael ST. A white matter stroke model in the mouse: axonal damage, progenitor responses and MRI correlates. *J Neurosci Methods* 2009; **180**: 261–272.
24 Tennant KA, Asay AL, Allred RP, Ozburn AR, Kleim JA, Jones TA. The vermicelli and capellini handling tests: simple quantitative measures of dexterous forepaw function in rats and mice. *J Vis Exp* 2010, piii: 2076; doi:10.3791/2076.
25 Belayev L, Saul I, Curbelo K, Busto R, Belayev A, Zhang Y *et al.* Experimental intracerebral hemorrhage in the mouse: histological, behavioral, and hemodynamic characterization of a double-injection model. *Stroke* 2003; **34**: 2221–2227.
26 MacLellan CL, Silasi G, Poon CC, Edmundson CL, Buist R, Peeling J *et al.* Intracerebral hemorrhage models in rat: comparing collagenase to blood infusion. *J Cereb Blood Flow Metab* 2008; **28**: 516–525.
27 MacLellan CL, Silasi G, Auriat AM, Colbourne F. Rodent models of intracerebral hemorrhage. *Stroke* 2010; **41**(10 Suppl): S95–S98.
28 Auriat AM, Wowk S, Colbourne F. Rehabilitation after intracerebral hemorrhage in rats improves recovery with enhanced dendritic complexity but no effect on cell proliferation. *Behav Brain Res* 2010; **214**: 42–47.
29 Wells JE, Biernaskie J, Szymanska A, Larsen PH, Yong VW, Corbett D. Matrix metalloproteinase (MMP)-12 expression has a negative impact on sensorimotor function following intracerebral haemorrhage in mice. *Eur J Neurosci* 2005; **21**: 187–196.
30 Hartman R, Lekic T, Rojas H, Tang J, Zhang JH. Assessing functional outcomes following intracerebral hemorrhage in rats. *Brain Res* 2009; **1280**: 148–157.
31 Felberg RA, Grotta JC, Shirzadi AL, Strong R, Narayana P, Hill-Felberg SJ *et al.* Cell death in experimental intracerebral hemorrhage: the 'black hole' model of hemorrhagic damage. *Ann Neurol* 2002; **51**: 517–524.
32 Liang H, Yin Y, Lin T, Guan D, Ma B, Li C *et al.* Transplantation of bone marrow stromal cells enhances nerve regeneration of the corticospinal tract and improves recovery of neurological functions in a collagenase-induced rat model of intracerebral hemorrhage. *Mol Cells* 2013; **36**: 17–24.
33 Carter AR, Astafiev SV, Lang CE, Connor LT, Rengachary J, Strube MJ *et al.* Resting interhemispheric functional magnetic resonance imaging connectivity predicts performance after stroke. *Ann Neurol* 2010; **67**: 365–375.
34 Jang SH, Kwon YH, Lee MY, Lee DY, Hong JH. Difference of neural connectivity for motor function in chronic hemiparetic stroke patients with intracerebral hemorrhage. *Neurosci Lett* 2012; **531**: 80–85.

Supplementary Information accompanies the paper on the Journal of Cerebral Blood Flow & Metabolism website (http://www.nature.com/jcbfm)